Proceedings of the 9th International Conference on Structural Dynamics, EURODYN 2014
Porto, Portugal, 30 June - 2 July 2014
A. Cunha, E. Caetano, P. Ribeiro, G. Müller (eds.)
ISSN: 2311-9020; ISBN: 978-972-752-165-4

Vibro-acoustic finite element analysis of a Permanent Magnet Synchronous Machine

Alex McCloskey[1], Xabier Arrasate[1], Gaizka Almandoz[2], Xabier Hernandez[3], Oscar Salgado[4]
[1]Department of Mechanical Eng., Faculty of Engineering, Mondragon Unibertsitatea, Loramendi 4, 20500 Arrasate/Mondragón, Spain
[2]Department of Electrical Eng., Faculty of Engineering, Mondragon Unibertsitatea, Loramendi 4, 20500 Arrasate/Mondragón, Spain
[3]Department of Mechanical Eng., Orona EIC, Polígono Lastaola, 20120 Hernani, Spain
[4]Department of Mechanical Engineering, Ik4 Ikerlan, Pº J. M.Arizmendiarrieta 2, 20500 Arrasate-Mondragón, Spain
email: amccloskey@mondragon.edu, jarrasate@mondragon.edu, galmandoz@mondragon.edu, xhernandez@orona-group.com, osalgado@ikerlan.es

ABSTRACT: Noise and vibration of electrical machines is a major concern. Changes in the machine design to improve its efficiency can lead to unacceptable vibrations. Tools to predict its vibratory and acoustic performance at the design stage need to be developed. An improved finite element model has been developed to analyse the vibration behaviour of a Permanent Magnet Synchronous Machine of a lift installation using the finite element software ABAQUS. All components and subsets of the machine have been modelled and validated by experimental modal analysis (EMA) performed on them. Some modelling issues have been overcome so that an accurate enough model has been reached. The laminated stator, as it is formed by a pack of several steel sheets, has been treated as an orthotropic material. Windings have been considered as a solid orthotropic part as well. The rotor and the stator and end-shields assemblies have also been validated comparing the calculated natural frequencies and modes shapes and those obtained by EMA. The bearings that join the rotor to the assembly of the stator have been represented by radial springs. The electromagnetic forces are applied in order to obtain the vibration response of the mechanical model. These forces are obtained from the magnetic air-gap flux density which has been obtained with a 2D finite element model developed by FLUX. Then, the vibration response has been used to calculate the radiated noise with an acoustic model in Virtual.Lab. The results given by the acoustic numerical model are compared with sound power measurements made in an anechoic chamber.

KEY WORDS: Permanent magnet synchronous motor (PMSM); Vibrations; Forced response; Electromagnetic noise.

1 INTRODUCTION

An improved finite element model is developed to calculate the vibro-acoustic response of a Permanent Magnet Synchronous Machine. Years ago the increasing use of inverters introduced more excitation harmonics which originated vibration and noise problems. Noise and vibration have a direct influence on users' perception of quality and comfort. Nowadays, in order to reduce costs, the efficiency of the machine needs to be improved and the quantity of magnets has to be minimised, as these materials are becoming more and more expensive. Because of this, it is really important to optimise the geometry of the stator, being the vibration behaviour a restriction, as some geometry modifications can lead to unacceptable vibrations.

Noise and vibration in electric motors have different origins that can be classified in three groups:

- Electromagnetic noise: Originated by magnetic forces acting on the stator and rotor
- Mechanical noise: Originated by bearings, shaft misalignment…
- Aerodynamic noise: Originated by the cooling fan.

The contribution of these sources changes depending on the working conditions. In the analysed case due to the absence of a fan the aerodynamic noise does not exist, so the generated noise is electromagnetic and mechanical. According to Gieras et al. [2] and Timar and Lai [5], mechanical and aero-dynamical noises increase with speed. However, Timar and Lai [5] affirm that in the very-low-speed domain mechanical and electromagnetic noises are present. The presence of mechanical noise at low speed machines is usually related to unhealthy mechanical elements. Other authors as Kawasaki et al. [3] assess that "noise below 1000Hz is due to radial electromagnetic excitation" and according to Lakshmikanth et al. [4], the electromagnetic source is the dominating source in low to medium power rated machines.

As in the analysed machine the rotational speed of the motor is low, for a healthy machine mechanical noise should be low, so the analysis is focused on the electromagnetic noise calculation.

For this task a structural finite element model needs to be developed which will be validated by experimental modal analysis (EMA).

In order to model the electric motor some modelling issues need to be overcome so that an accurate enough model is reached.

First, the laminated stator presents different stiffness in radial and axial directions, according to Gieras et al. [2], Verdyck and Belmans [6] and Wang and Lai [7], as it is formed by a pack of several steel sheets. Thus, orthotropic material properties are applied to the solid part representing the laminated stator. Those properties are adjusted according to the experimental results as that stiffness depends on the compression pressure acting in the axial direction (Wang and Williams [8] and Watanabe et al. [9]) during manufacturing and the procedure used to tie these pack of steel sheets and, therefore, is hard to determine.

Then, different modelling strategies are found in literature for the windings. Belmans et al. [1] and Wang and Lai [7] consider that the mass supplement due to windings is more

important than the supplementary stiffness, so windings are treated as additional masses. However, it is hard to know if this strategy might be applicable for any stator geometry. So according to Gieras et al. [2], the volume of material representing the stator windings, which fills the slots of the stator, is also modelled as a solid part. Its orthotropic properties are again estimated according to the experimental modal analysis results.

When more parts are added, the junctions have to be analysed taking the results obtained by EMA into account. The initial approach is to consider that one part is glued to the other, so that the coupling between them is stiffer than real.

Finally, for the complete motor model the most complicate aspect is the mounting of the rotor, which is modelled introducing radial springs where the bearings are placed.

2 EXPERIMENTAL ANALYSIS

2.1 Modal testing set-up and procedure

The modal testing equipment consists on:

- Acquisition system: 2 Brüel & Kjaer Front-ends and laptop with Pulse Labshop software.
- Impact hammer
- 10 triaxial accelerometers.

The system is elastically suspended by rubber bands to avoid the effect of constraints in the natural modes of the system.

For each analysed system a different discretisation is used resulting in different number and position of measurement points. The analysed systems or components are:

- Laminated stator.
- Laminated stator and windings.
- Laminated stator, windings and end-shields assembly.
- Rotor and shaft assembly.
- The previous two assemblies mounted with the corresponding bearings.

2.2 Vibration measurement under operating conditions

The vibration measurements under operating condition are carried out for the complete motor mounted on a support using the same equipment as for the modal testing excepting the hammer which obviously is not needed for these measurements.

The motor is almost the same as the last system analysed by modal testing, except for the brake that is mounted for the operating measurements. In the modal analysis of the machine, this is composed by the stator, windings and end-shields assembly where the rotor and shaft assembly is mounted by bearings. The brake is not mounted, as the aim of that modal analysis is mainly to characterise the bearings and their stiffness and therefore it is necessary to measure the acceleration in different points of the shaft. As the brake blocks the way to the shaft and thus, it is not possible to place accelerometers on it, the modal analysis is carried out without the brake. Otherwise, at the measurements under operating conditions the whole machine is analysed, so that in this case no accelerometers are placed at the shaft. Nevertheless, the rest of the measurement points are the same as in the modal analysis except some accelerometers that in the modal analysis are placed in the base and in the operating condition measurements it is not possible.

It is assumed that there will not be a big difference between the machine of the modal analysis and the machine that is used in the operational measurements, as the contribution of the brake is mainly of a mass supplement to the system.

The machine operates in no load condition.

2.3 Acoustic power measurement under operating conditions

The acoustic power is measured in a semi-anechoic chamber, in the same place where the vibration measurements were carried out, where eight microphones are placed around the machine. These eight microphones are placed at 1 metre from the machine in an imaginary parallelepiped around it. From the sound pressure measured at these eight points the acoustic power is obtained following the standard ISO 3746.

The machine operates in the same conditions as in the vibration measurements.

3 STRUCTURAL FINITE ELEMENT MODEL

The structural finite element model was developed validating experimentally each of the main components as it is listed below. To reduce the amount of results and taking into account that this analysis is focused on low frequencies, as it was commented at the introduction, just modes below 1000 Hz are shown.

3.1 Stator model

This component is hard to model as it is formed by a pack of several steel sheets and thus its mechanical properties need to be considered as orthotropic. This implies the necessity of determining those properties and for this purpose an updating of the unknown properties was made according to the experimental results using Virtual.Lab optimisation module.

The resulting properties are 7800 kg/m^3 density, 200 GPa normal elasticity modulus and 50 GPa shear modulus in the sheets' plane; 6 GPa elasticity modulus in the axial direction and 4.1 GPa shear modulus; and 0.2546 Poisson ratio in the plane of the sheets and 0.0052 Poisson ratio respect to the axial direction.

Applying those mechanical properties the modes obtained by the FE model are shown in Figure 1.

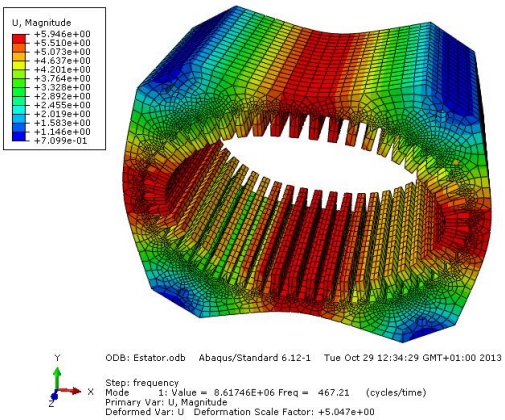

a)

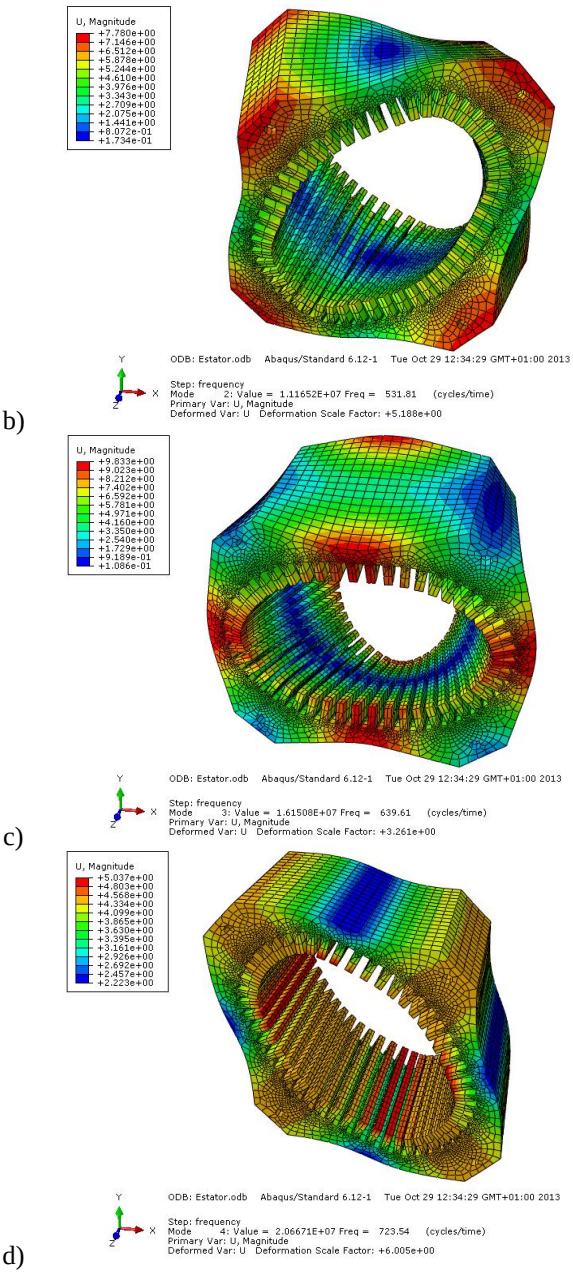

Figure 1. Stator vibration modes: (a), first mode; (b), second mode; (c), third mode; (d), fourth mode.

The calculated and the experimentally obtained natural frequencies are compared at Table 1.

Table 1. Stator natural frequency comparison.

	Experimental	FEM	Relative error (%)
Mode 1	488.7	467.21	4.39
Mode 2	497.4	531.81	6.92
Mode 3	661.4	639.61	3.29
Mode 4	746.2	723.54	3.04

3.2 Stator and windings model

The windings are even a harder part of the motor to model as they are composed of copper wires covered by an insulating material which avoids electric currents between them. Similarly to the laminated stator, the volume of the windings which fills the stator slots (see Figure 2) has been considered as a solid part assigning an orthotropic mechanical properties material.

In the FE model this part is glued to the stator part using the constraint "tie" provided by ABAQUS, which sticks the nodes of the slave surface to the elements of the master surface. This assembly is shown in Figure 2.

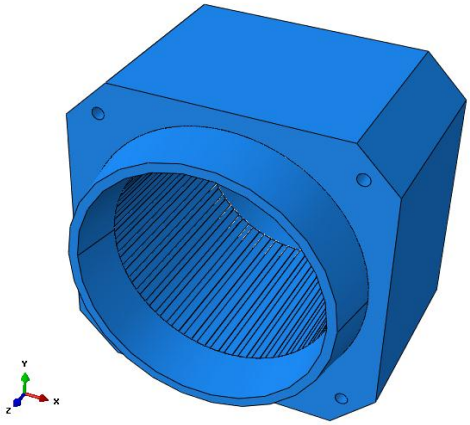

Figure 2. Stator and windings model

Again, the mechanical properties of the part representing the windings are adjusted according to the experimental results by an optimisation process carried out by Virtual.Lab optimisation.

The model updating process has led to errors in the modes below 1000 Hz of less than 6 %. However, the relative error obtained for the first vibration mode was over 5% and another updating process has been carried out focused in lowering the relative error of this mode and the third. The aim of this process is to improve the accuracy on determining the in-plane modes, the mode shapes that present no deformation in the axial direction (see modes 1 and 3 in Figure 3). The reason for improving the accuracy of the in-plane modes is that end-shields constraint axial deformations and thus, the modes presenting axial deformations become less important on those assemblies at the analysed frequency range (see Figure 5).

The following mechanical properties are obtained for the windings part: 20 GPa elasticity modulus in the axial direction and 0.6 GPa in the others; 4.3 GPa the in-plane (the plane of the steel sheets) shear modulus and 10 GPa in the other directions; 0.021 Poisson ratio in the plane of the steel sheets and 0.3403 in the other planes; and a density of 3500 kg/m^3. These properties result in the mode shapes shown in Figure 3.

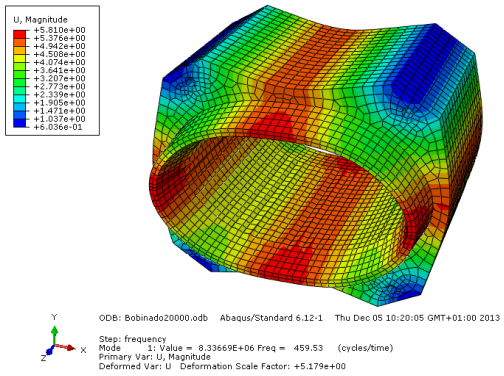

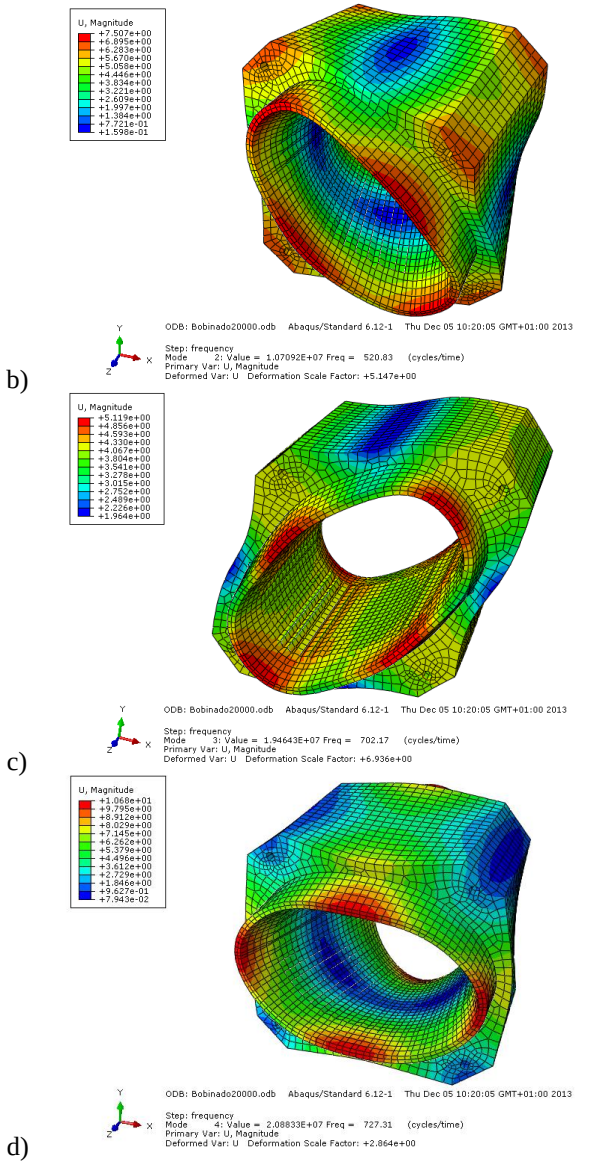

Figure 3. Stator and windings vibration modes: (a), first mode; (b), second mode; (c), third mode; (d), fourth mode.

The calculated and the experimentally obtained natural frequencies are compared at Table 2. It has to be underlined that the relative error obtained for the in-plane modes is below 3%, being these modes, as it was explained before, the important ones when the other parts are assembled.

Table 2. Stator and windings model natural frequency comparison.

	Experimental	FEM	Relative error (%)
Mode 1	449	459.53	2.34
Mode 2	560.4	520.83	7.06
Mode 3	714	702.17	1.66
Mode 4	790.3	727.31	7.97

3.3 Stator, windings and end-shields

This model adds to the stator and windings system the end-shields, those parts where the different components of the motor are mounted. As it can be seen in Figure 4, one of these two parts is the cover of the motor at one of the sides of the stator. In this part the bearing of that side of the shaft is mounted. The other part holds the stator and rotor at one side and the brake at the other side, leaving the pulley in the middle. This part is also the base of the entire motor.

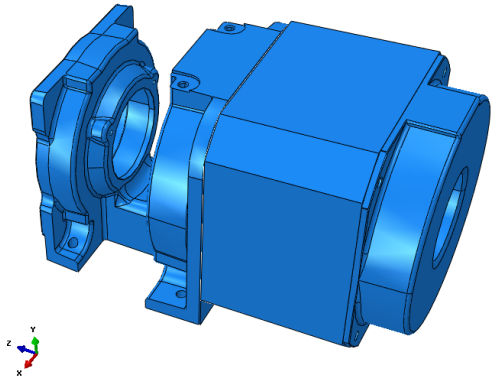

Figure 4. Stator assembly: Stator, windings and end-shields.

These two parts are screwed to the stator and it is considered that this join is strong enough to be modelled as if the contact surface pair was welded. Thus, "tie" ABAQUS constraint is used again to join these parts.

The material of these two parts is the grey cast iron EN-GJL-250 (GG-25), whose mechanical properties are 7200 kg/m^3 density, 110 GPa elasticity modulus and 0.26 Poisson ratio.

In Figure 5 the modes obtained for the described model are shown.

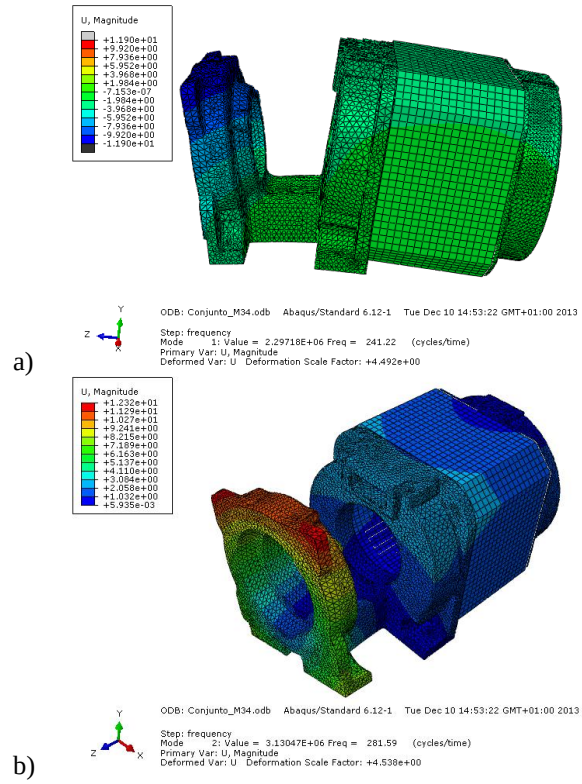

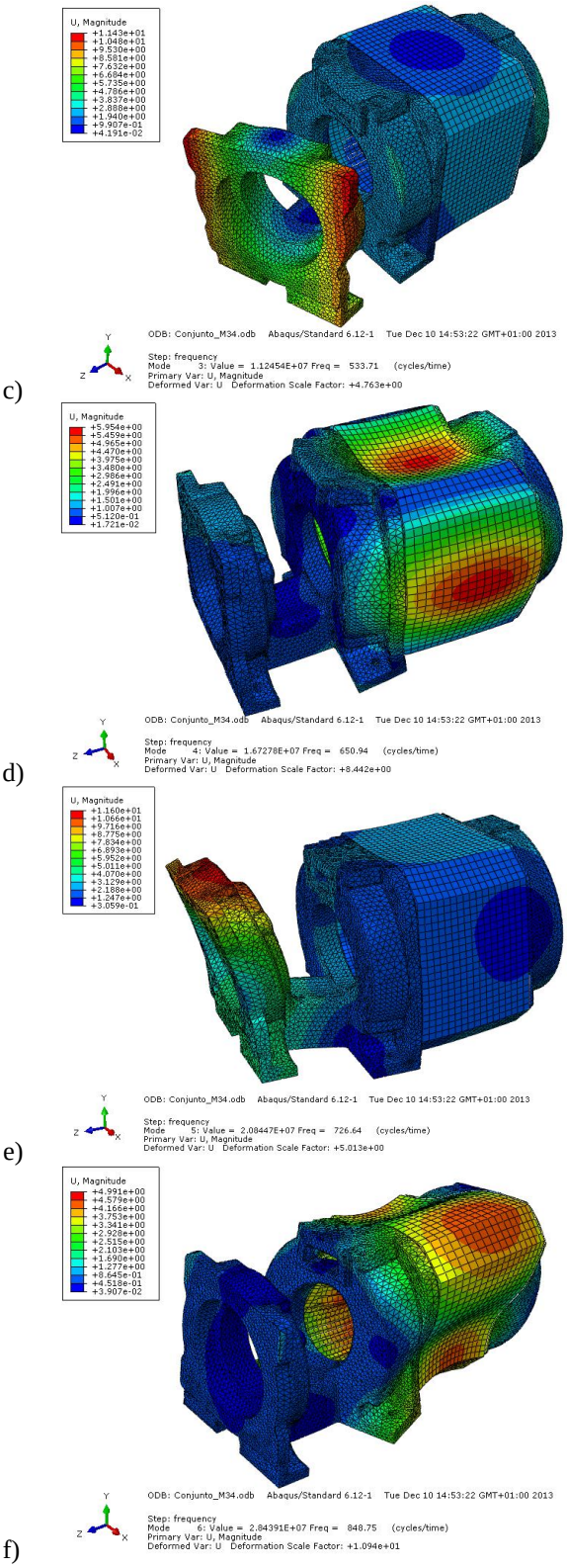

Figure 5. Stator, windings and end-shields vibration modes: (a), first mode; (b), second mode; (c), third mode; (d), fourth mode; (e), fifth mode; (f), sixth mode.

Comparing these results with the modes obtained by the EMA the relative errors are obtained for each mode as shown in Table 3. There can be seen that this assembly is modelled accurately as the biggest relative error is around 5%.

Table 3. Stator, windings and end-shields model natural frequency comparison.

	Experimental	FEM	Relative error (%)
Mode 1	232.75	241.22	3.64
Mode 2	275.45	281.59	2.23
Mode 3	528.29	533.71	1.03
Mode 4	618.9	650.94	5.18
Mode 5	730.06	726.64	0.47
Mode 6	878.59	848.75	3.40

3.4 Rotor and shaft model

This model is the assembly of the shaft and the rotor (see Figure 6). Again, it is considered that both parts are rigidly joined, so "tie" ABAQUS constraint is used to connect them. The shaft is a steel solid part, so its isotropic properties are 7800 kg/m^3 density, 210 GPa elasticity modulus and 0.3 Poisson ratio. Otherwise, the rotor is similar to the stator and therefore orthotropic properties need to be applied. In this case the properties are: 10 GPa elasticity modulus in the axial direction and 210 GPa in the others; 78 GPa the in-plane (the plane of the steel sheets) shear modulus and 40 GPa in the other directions; 0.3 Poisson ratio in the plane of the steel sheets and 0.01 in the other planes; and the same density as the steel of the shaft, 7800 kg/m^3.

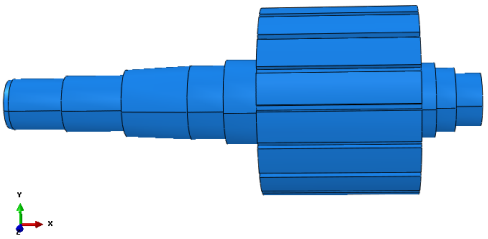

Figure 6. Shaft and rotor assembly model.

The modes obtained for the proposed model are shown in Figure 7.

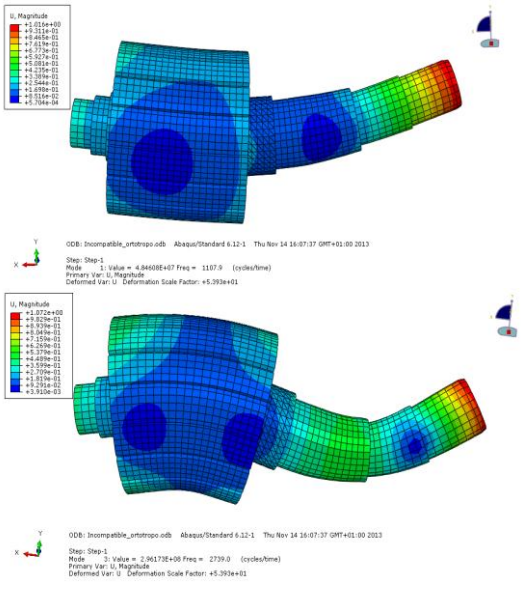

Figure 7. Rotor and shaft vibration modes: (a), first mode; (b), second mode.

The relative errors for these modes are given in Table 4. The shown two modes are at higher frequencies than the frequency range under analysis, but at least, those two modes are useful to see the agreement between experimental and simulated results.

Table 4. Rotor and shaft model natural frequency comparison.

	Experimental	FEM	Relative error (%)
Mode 1	1199.9	1107.9	7.66
Mode 2	2484.7	2739	10.23

3.5 *Complete motor system excluding the brake and the pulley*

The rotor and shaft assembly is introduced inside the stator, windings and end-shields assembly (see Figure 8) and both assemblies are joined by springs. Each bearing is modelled by four springs and the stiffness of the springs is adjusted according to the modes obtained by EMA. This stiffness is 50000 N/mm for each spring.

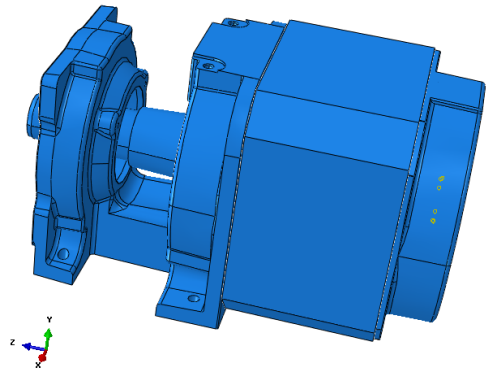

Figure 8. Stator and rotor assembly model.

With the mentioned modelling of the bearings the modes obtained by the EMA and the ones calculated by FEM are compared and the relative errors for each mode are calculated. In Table 5 the relative errors are shown and it has to be remarked that most modes are predicted accurately. The exceptions are the two modes of the stator that were not visualized at the EMA and some modes of the rotor that were hard to identify. Due to the difficulty to place accelerometers on the rotor too few measurements points were located on it and this lack of information make some modes (like the sixth one) hard to compare.

Table 5. Stator and rotor natural frequency comparison.

	Experimental	FEM	Relative error (%)
Mode 1	270,76	264,09	2,55
Mode 2	294,07	305,62	3,93
Mode 3	297,41	321,21	8
Mode 4	569,42	550,94	3,24
Mode 5	603,51	611,49	1,32
Mode 6	699,62	572,46	18,17
Mode 7	-	667,3	-
Mode 8	775,8	795,37	2,55
Mode 9	-	855,16	-

3.6 *Complete motor system*

The brake and the pulley are added to this final model (see Figure 9). These parts are assembled in the same way as in the previous assemblies, considering that they are joined to the other parts rigidly. Therefore, the contact surfaces between those parts are glued using again the ABAQUS "tie" constraint.

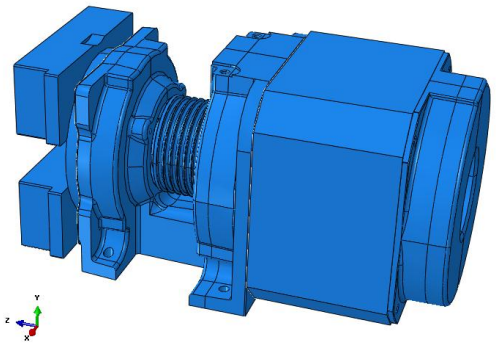

Figure 9. Complete machine model.

This model is not compared with experimental data as its experimental modal analysis was not carried out.

4 VIBRATION RESPONSE CALCULATION

4.1 *Electromagnetic forces calculation*

The magnetic pressure distribution in the surface of a tooth and in the surface of a pole is calculated by FEM (FLUX 2D software) for the period of time corresponding to the fundamental frequency. In Figure 10 the magnetic pressure obtained for the tooth surface is shown.

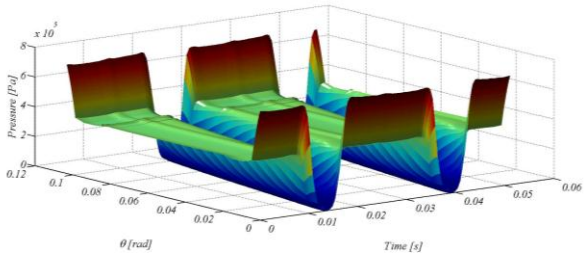

Figure 10. Magnetic pressure on the tooth surface.

Then, the magnetic pressure was decomposed obtaining the most important frequency components by FFT.

For the tooth the values of the component orders are plotted (see Figure 11) and using the seven most important components the pressure can be accurately reconstructed as it is shown in Figure 12.

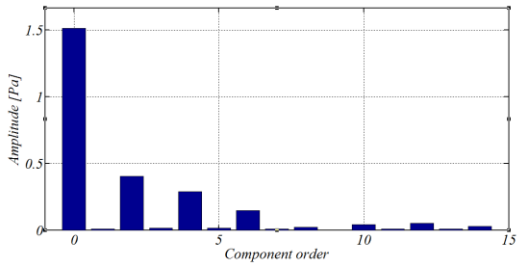

Figure 11. Pressure spectrum in a tooth.

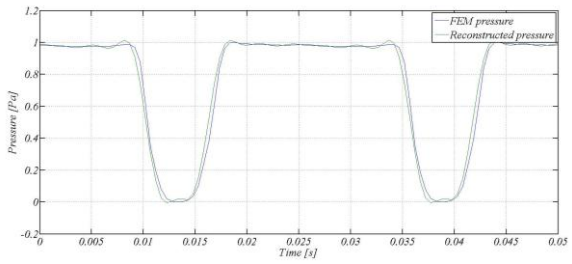

Figure 12. Original magnetic pressure evolution in time vs. reconstructed pressure.

And for a pole the amplitudes of the component orders are obtained and shown in Figure 13. Taking the four most considerable components into account the pressure is accurately reconstructed as it is shown in Figure 14.

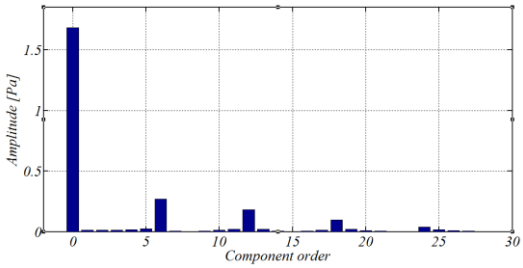

Figure 13. Pressure spectrum in a pole.

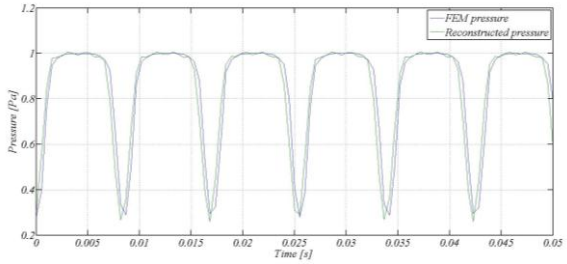

Figure 14. Original magnetic pressure evolution in time vs. reconstructed pressure.

4.2 Electromagnetic forces application to the structural model and vibration response validation

The most relevant electromagnetic pressure frequency components are introduced as a pressure load in the ABAQUS structural model and by the modal superposition procedure the vibration response is calculated.

The operating conditions measurements are used to verify the calculated dynamic response of the machine, choosing for the comparison the nominal speed and no load condition. In Figure 15 the acceleration in the centre of the stator in the face pointing upwards is compared with the experimental measurements for the three directions. This measurement point was chosen as the centre of the stator is the most meaningful position in terms of vibration due to electromagnetic exciting forces.

About the results obtained, it has to be pointed out that the main difficulty to verify these calculations was the uncertainty introduced by the support where the machine is mounted. This support is not completely rigid so the base of the machine has to be tied allowing some flexibility. However the springs placed in the base for this purpose have not given good enough results for all direction as it can be seen in Figure 15.

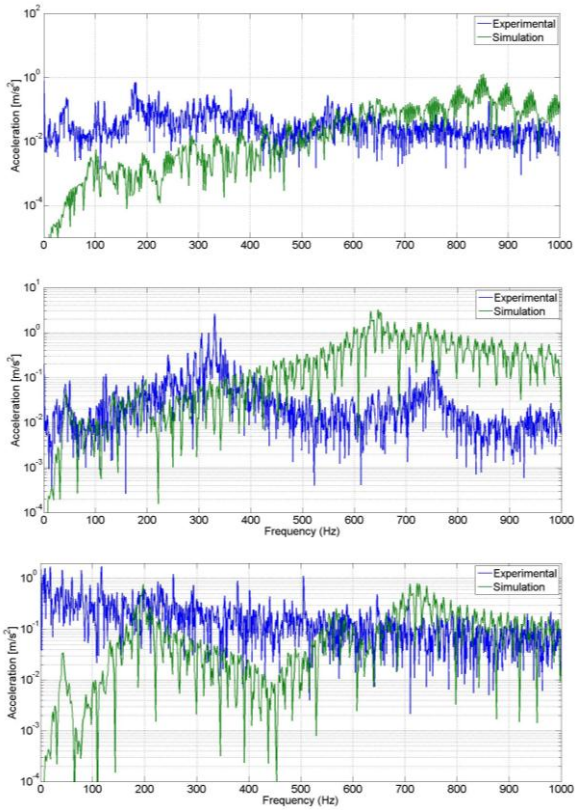

Figure 15. Acceleration in m/s^2 in the centre of the stator comparison, simulated vs. experimental: (a), in horizontal direction perpendicular to the axial; (b), in normal direction to the surface, so in vertical direction; (c), in axial direction.

5 ACOUSTIC RESPONSE CALCULATION

5.1 Acoustic finite element model

The motor finite element model is imported in Virtual.Lab and between the skin of this model and a surrounding shell called "Convex mesh" the air mesh is introduced. The properties given to the air are the density which is 1.225 kg/m^3 and the speed of sound which is 340 m/s. Then, "Automatically Match Layer (AML)" property is applied to the external surface of the air which applies the Sommerfeld condition that imposes to that surface to be a non-reflective boundary.

The previously calculated vibration accelerations, which could also be velocities or displacements, are applied as boundary condition to this acoustic model.

5.2 Acoustic power calculation and experimental validation

The acoustic power is obtained by the model explained previously and then the results are compared with the acoustic power obtained experimentally. These results are shown in Figure 16 and as it is sensible, introducing accelerations which are not accurate enough leads to an acoustic power quite over the real one, especially at high frequencies.

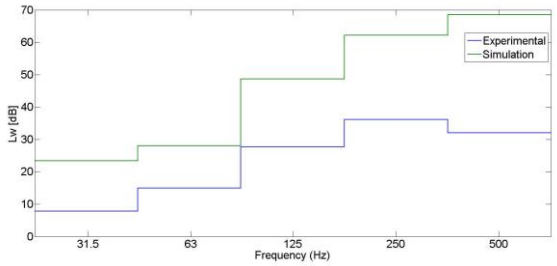

Figure 16. Acoustic power comparison, simulated vs. experimental.

6 CONCLUSIONS

The first conclusion to be pointed out is that, as it was observed in the literature, the main modelling issue is to determine the mechanical properties of the laminated components as the stator and the rotor and specially the windings.

In the case of the laminated stator and rotor some values can be found at the literature that applied to the solid orthotropic part may give good agreement with the experimental behaviour. However, for windings there are almost as many modelling strategies as publications about electric motors vibratory behaviour and as different windings topologies can be found. The strategy of modelling the windings as a solid orthotropic part was chosen as it is the most conservative one as it avoids making uncertain assumptions as considering that windings are just an added mass. Giving orthotropic properties to the solid part representing the windings has given good results as the mechanical properties were adjusted according to the experimental modal analysis so that the real behaviour was modelled.

At this point, it is important to remark that the accuracy at predicting some modes may not be important to obtain a reliable dynamic response calculation. This can happen with the modes of the stator and windings system that present deformations along the axial direction. The properties in the axial direction are difficult to estimate and it is hard to adjust them by an optimisation process as it was seen at this work. However, it was shown that those modes when the covers are added, when the stator is joined to the end-shields, tend to increase their natural frequencies and therefore they become less important for the accuracy of the dynamic response calculation.

The next issue to overcome has been the interaction between different parts or how the different parts are joined one to each other. At the parts that are screwed the join was considered strong enough so that the contact surfaces are glued. This assumption is shown to be valid as the modes obtained at the calculation are really close to those obtained experimentally.

Nevertheless, there is a harder interaction to model which is the bearings connecting the shaft and rotor assembly to the stator and end-shields assembly. To model these bearings springs are used placing four of them with a 90 degrees angle between them in the centre of the contact surface of each of the bearings. This modelling strategy gives good results as the bearings used are one row deep groove ball bearings that can be considered as a simple support in the centre of the bearing. Therefore the rotation is not restraint at that point which would be another uncertainty to model at double row ball bearings or at roller bearings.

About the forced response calculation the most remarkable conclusion is that to validate the finite element model properly the machine acceleration should be measured rigidly tied to the floor. From this acceleration a proper comparison can be made with the simulation of the machine rigidly tied in its base and then the model will be validated. This future work is important to ensure that the mesh of the finite element model is good enough and therefore that the mesh is not the source of the obtained error.

Analysing the acoustic power comparison it is even more necessary to check the dynamic response calculation as the difference between the calculated acoustic power and the measured is quite big. This difference makes sense according to the accelerations as the main contribution to the acoustic power is made by the accelerations normal to the surface. Analysing that acceleration shown in Figure 15, it can be seen that the difference increases as frequency increases, the same that happens with the acoustic power. Therefore, an improvement of the acoustic power estimation is expected, once the vibration calculation is verified for the same boundary conditions correcting the uncertainties or badly defined aspects.

ACKNOWLEDGMENTS

The work presented in this paper has been carried out with the generous support of the company Orona EIC and the Basque Government (SIRUMA, S-PE12MU010, and HESIVAMO, UE2013-05).

REFERENCES

[1] Ronnie JM Belmans, Dirk Verdyck, Willy Geysen, and Raymond D Findlay. Electromechanical analysis of the audible noise of an inverter-fed squirrel-cage induction motor. IEEE Transactions on Industry Applications, 27 (3), 539–544, 1991.

[2] Jacek F Gieras, Chong Wang, and Joseph Cho Lai. Noise of polyphase electric motors. CRC press, 2005.

[3] Ryo Kawasaki, Yasuo Hironaka, and Masaharu Nishimura. Noise and vibration analysis of elevator traction machine. In INTER-NOISE and NOISE-CON Congress and Conference Proceedings, 369–377. Institute of Noise Control Engineering, 2010.

[4] S. Lakshmikanth. Noise and vibration reduction in Permanent Magnet Synchronous motors–A review. International Journal of Electrical and Computer Engineering (IJECE), 2 (3), 405–416, 2012.

[5] PL Timar and JCS Lai. Acoustic noise of electromagnetic origin in an ideal frequency-converter-driven induction motor. IEE Proceedings-Electric Power Applications, 141 (6), 341–346, 1994.

[6] D. Verdyck and R.J.M. Belmans. An acoustic model for a permanent magnet machine: modal shapes and magnetic forces. IEEE transactions on industry applications, 30 (6), 1625–1631, 1994.

[7] C. Wang and JCS Lai. Vibration analysis of an induction motor. Journal of sound and vibration, 224 (4), 733–756, 1999.

[8] Huan Wang and Keith Williams. The vibrational analysis and experimental verification of a plane electrical machine stator model. Mechanical Systems and Signal Processing, 9 (4), 429–438, 1995.

[9] S. Watanabe, S. Kenjo, K. Ide, F. Sato, and M. Yamamoto. Natural frequencies and vibration behaviour of motor stators. IEEE Transactions on Power Apparatus and Systems, (4), 949–956, 1983.